Acta Cryst. (1998). D**54**, 1456–1459

Production, crystallization and diffraction to atomic resolution of an antibody Fv specific for the blood-group A oligosaccharide antigen

Sonia I. Patenaude,[a] C. Roger MacKenzie,[b] Doris Bilous,[b] Rebecca J. To,[b] Stephen E. Ryan,[a] N. Martin Young[b] and Stephen V. Evans[a]* at [a]*Department of Biochemistry, University of Ottawa, 451 Smyth Road, Ottawa, Ontario K1H 8M5, Canada, and* [b]*Institute for Biological Sciences, National Research Council of Canada, 100 Sussex Drive, Ottawa, Ontario K1A 0R6, Canada. E-mail: evans@uottowa.ca*

(*Received 26 January 1998; accepted 20 April 1998*)

Abstract

The histoblood-group ABO carbohydrate antigens are well known as important factors in blood transfusions, but they can also act as receptors for infectious agents and have been implicated in susceptibility to certain carcinomas. A single-chain variable-domain antigen-binding fragment (scFv) gene based on the known sequence of an anti-blood-group-A monoclonal antibody (AC1001) has been synthesized and expressed in *Escherichia coli*. The purified scFv preparation existed primarily in the monomeric form but also contained large amounts of dimeric and higher oligomeric forms. The corresponding variable-domain antigen-binding fragment (Fv) was generated by cleaving the V_L–V_H linker with subtilisin, and its activity was demonstrated by surface plasmon resonance with an immobilized bovine serum albumin A–trisaccharide conjugate (K_D = 290 μM). AC1001 Fv crystals grown in the presence of *N*-acetylgalactosamine diffracted to 0.93 Å resolution. This is the first reported example of a crystal of an antibody antigen-binding fragment diffracting to atomic resolution.

1. Introduction

The carbohydrate structures of glycoconjugates found on cell surfaces are important factors in discrimination between self and non-self. One of the first types of these cell-surface antigens to be reported was the histoblood-group ABO, which consists of three carbohydrate antigens, A, B and H. These chemical moieties are anchored to erythrocyte membranes by glycoproteins or sphingolipids and are also widely distributed throughout the body (Tizzard, 1984; King, 1994; Garratty, 1995). ABO mismatch is the primary reason for the failure of blood transfusions. In more recent years the blood-group antigens have received renewed interest as putative receptors for bacterial and viral agents, and have been linked to the susceptibility and progression of certain carcinomas (Garratty, 1995).

The A and B blood-group antigens are synthesized in the body by corresponding glycosyltransferases, which catalyse the addition of monosaccharides to the precursor H molecule (King, 1994). Glycosyltransferase A attaches GalNAc in an α-1,3 linkage to the terminal Gal of the H antigen to form the A antigen, D-GalNAcα1,3(L-Fucα1,2)D-Galβ1,3/4GlcNAc, while the α-1,3 addition of Gal onto H by glycosyltransferase B forms the B antigen, D-Galα1,3(L-Fucα1,2)D-Galβ1,3/4GlcNAc (Tizzard, 1984). Interestingly, although the A and B antigens differ only in the substitution of an acetamido for a hydroxyl group, this small change in chemical structure can have serious serological impact. Anti-A and/or anti-B antibodies are almost always present in high concentrations in persons lacking the corresponding erythroid antigen, and rapid onset of a transfusion reaction will occur if the host's serum antibodies recognize an antigen presented by transfused red blood cell. This causes the rapid agglutination of erythrocytes, as well as activation of complement, leading to massive intravascular haemolysis (Seymour *et al.*, 1995). If left untreated, mismatched blood transfusion can cause death.

Determination of the molecular structure of anti-blood-group antibodies may lead to a greater understanding of the mechanism by which these proteins discriminate between the largely similar carbohydrate structures of the A and B antigens, the types of interactions involved in cell–cell and cell–pathogen recognition, the mechanisms of viral and bacterial infections involving blood-group antigens and the statistical association between blood-group antigens and certain carcinomas. The only other structure of an anti-blood-group antibody fragment reported to date is the 3.0 Å structure of the unliganded Fab [fragment containing antibody variable-domain dimer fragment (Fv) and first constant-region domain dimer] to antibody CF4C4, specific for the Lewis *a* blood-group antigen (Vitali *et al.*, 1987).

To study the anti-blood-group-A antibody and its interaction with the A antigen, a single-chain Fv (AC1001 scFv) was produced based on the sequence of the anti-blood-group-A IgM hybridoma AC1001 (Chen *et al.*, 1987). The gene was assembled from segments of synthetic genes constructed to produce AC1001 Fab (MacKenzie *et al.*, 1994). ScFvs are recombinant polypeptides composed of variable light-chain (V_L) and variable heavy-chain (V_H) amino-acid sequences; the carboxyl terminus of one domain is linked to the amino terminus of the second by a peptide of sufficient length to bridge this distance (Bird *et al.*, 1988). This type of antigen-binding fragment was developed in order to avoid problems due to the association of the V_H and V_L domains of Fvs. The use of recombinant scFv also avoids the difficulty and product heterogeneity encountered in the isolation of Fab and Fv fragments from IgMs by proteolytic digestion, and will aid in planned site-directed mutagenesis studies.

The reported affinities of carbohydrate–antibody complexes are generally lower than those of antibodies for proteins, peptides and many small molecules. As a possible consequence, there have been reports of only two independent high-resolution crystal structures of antibody–antigen complexes for carbohydrate-specific antibodies (Cygler *et al.*, 1991; Zdanov *et al.*, 1994; Jeffrey *et al.*, 1995). To date there have been two reports of antibody-fragment crystals which scatter to 1.7 Å resolution (Zdanov *et al.*, 1994; Patenaude *et al.*, 1998),

ISSN 0907-4449

one report at 1.28 Å resolution (Ostermeier *et al.*, 1995), but no reports of crystals which scatter to atomic resolution (*i.e.* beyond 1.0 Å).

Here we describe the purification, crystallization and preliminary diffraction analysis at atomic resolution of an Fv specific for the blood-group-A antigen grown in the presence of GalNAc. The relatively large conserved regions of antibody antigen-binding fragments, combined with the sequence variability of the CDR loops, has made them a natural target for structure prediction. Significant success has been reported in predicting the conformations of individual CDR loops (Chothia & Lesk, 1987; Chothia *et al.*, 1989; Martin & Thornton, 1996; Al-Lazikani *et al.*, 1997). However, the nature of the domain association of V_L and V_H, which is key to the conformation of the antigen-binding site, remains difficult to predict. The AC1001 Fv offers the first opportunity to study the details of antibody loop conformation and domain association at the atomic level, and will provide necessary structural data for the next generation of predictive methods.

2. Experimental

2.1. *Gene construction*

A gene encoding a scFv version of AC1001 was assembled from previously synthesized Fd and L chain genes (MacKenzie *et al.*, 1994) using available restriction sites. Synthetic oligonucleotides encoding a $(GGGGS)_3$ linker were inserted between G117 of the L chain and Q1 of the H chain by restriction-enzyme digestion and ligation. A sequence encoding SGEQKLISEEDLNHHHHH, which contained the *c-myc* immunodetection tag (underlined) and a His5 purification tag, was inserted following residue 119A of the H chain using synthetic oligonucleotides and available restriction sites.

2.2. *Single-chain Fv purification and Fv generation*

The AC1001 scFv was expressed, detected and purified as previously described (MacKenzie *et al.*, 1994), except that a 0–500 m*M* imidazole gradient was used to elute the recombinant protein in immobilized metal-ion affinity chromatography. Size-exclusion chromatography (SEC) revealed that the scFv monomer was in equilibrium with the dimer and, to a smaller extent, trimer and tetramer. Although attempts were made to crystallize the intact scFv, crystals were only observed after the linker had been cleaved with subtilisin. This protease treatment also resulted in at least partial removal of the carboxyl-terminal extensions (*c-myc* immunodetection tag and His5 tail). To IMAC-purified scFv (2.5 mg ml^{-1}) was added 1 *M* Tris–HCl pH 8.0 and sodium azide to final concentrations of 0.1 *M* and 0.02%, respectively. To this sample mixture, subtilisin was added in a 1:500(*w*/*w*) ratio with AC1001 scFv; the reaction was carried out at 310 K for 5 h and stopped by adding 1:100(*v*/*v*) of 0.1 *M* phenylmethylsulfonyl fluoride in dimethyl sulfoxide. The digest was then dialyzed against phosphate-buffered saline (PBS) (10 m*M* sodium phophate pH 7.0 and 150 m*M* sodium chloride). SEC analysis revealed a single-molecular-weight species corresponding to the Fv (Fig. 1), showing that the linker peptide had been cleaved. A Superdex 75 HR 10/30 (Pharmacia Biotech) column was equilibrated with 2 bed volumes of PBS at a flow rate of 0.5 ml min^{-1}. The dialyzed sample was applied to the column in several 250 µl injections at the above flow rate and eluted in PBS. The major peaks corresponding to AC1001 Fv were collected, pooled and concentrated in a Centricon 10 (Amicon) to a final concentration of 7 mg ml^{-1}.

2.3. *Surface plasmon resonance*

Equilibrium binding data were collected using a BIACORE® 1000 instrument (Biacore Inc., Piscataway, NJ). Approximately 5000 RUs of bovine serum albumin (BSA) or BSA–A-trisaccharide (Chembiomed) were immobilized on research-grade CM5 sensor chips (Biacore, Inc.) using the amine-coupling kit supplied by the manufacturer. All measurements were performed in HEPES-buffered saline containing 10 m*M* HEPES pH 7.4, 150 m*M* NaCl, 3.4 m*M* EDTA and 0.005% Surfactant P-20 (Biacore, Inc.). Analyses were carried out at 298 K and at a flow rate of 10 µl min^{-1}. Values for equilibrium binding were derived by subtracting the control binding (BSA surfaces) from the active-surface binding (BSA–A-trisaccharide surfaces).

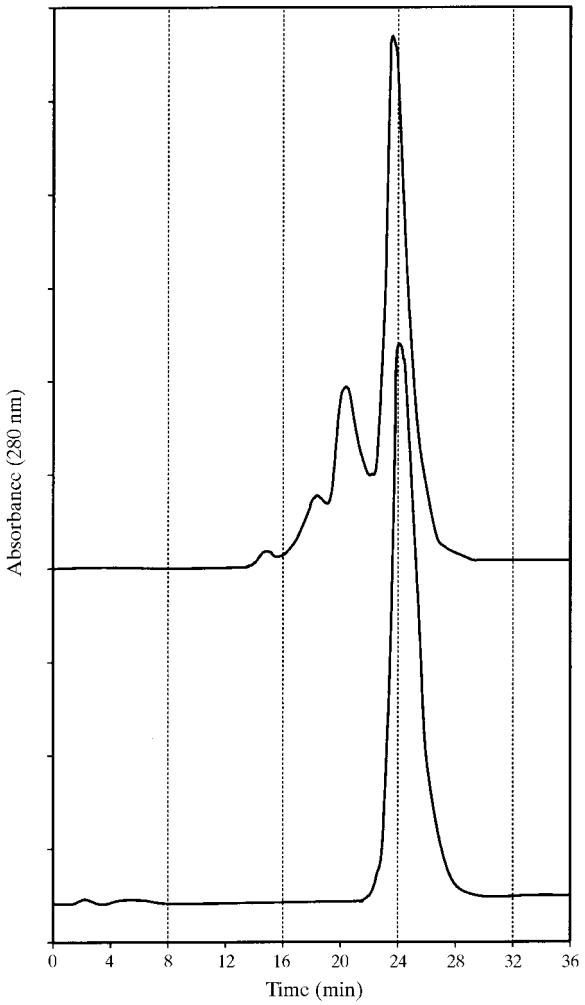

Fig. 1. Size-exclusion FPLC of AC1001 scFv obtained by IMAC (top trace) and AC1001Fv obtained by subtilisin treatment (bottom trace). From left to right are eluted the tetramer, trimer, dimer and scFv monomer.

2.4. *Crystallization and X-ray diffraction data collection*

Crystals of both AC1001 Fv and the AC1001 Fv–GalNAc complex were obtained using the hanging-drop vapour-diffusion method (McPherson, 1982). For the Fv–GalNAc complex, 4.5 µl of Fv (7 mg ml^{-1}) were mixed on a cover slip with 1 µl 900 m*M* GalNAc and 4.5 µl of reservoir solution, typically 30% PEG 4000, 0.1 *M* HEPES pH 7.0 and 10 m*M* $CaCl_2$, and equilibrated at room temperature over a 1 ml reservoir using a Linbro tissue-culture plate (Flow Labs). Crystals of ~0.5 × 0.3 × 0.3 mm were obtained within seven days following macroseeding, and grew to over 1 mm in a few weeks. The initial seed was obtained under similar conditions, but with a slightly higher PEG 4000 concentration. The unligated Fv (7 mg ml^{-1}) was mixed on a cover slip in a 1:1 ratio with reservoir solution (25–30% PEG 4000, 0.1 *M* HEPES pH 8.0 and 10 m*M* $CaCl_2$) and equilibrated at room temperature over a 1 ml reservoir using a Linbro tissue-culture plate. Crystals of at least 0.4 × 0.2 × 0.1 mm were obtained by macroseeding, the initial seed being obtained using slightly higher PEG 4000 concentration.

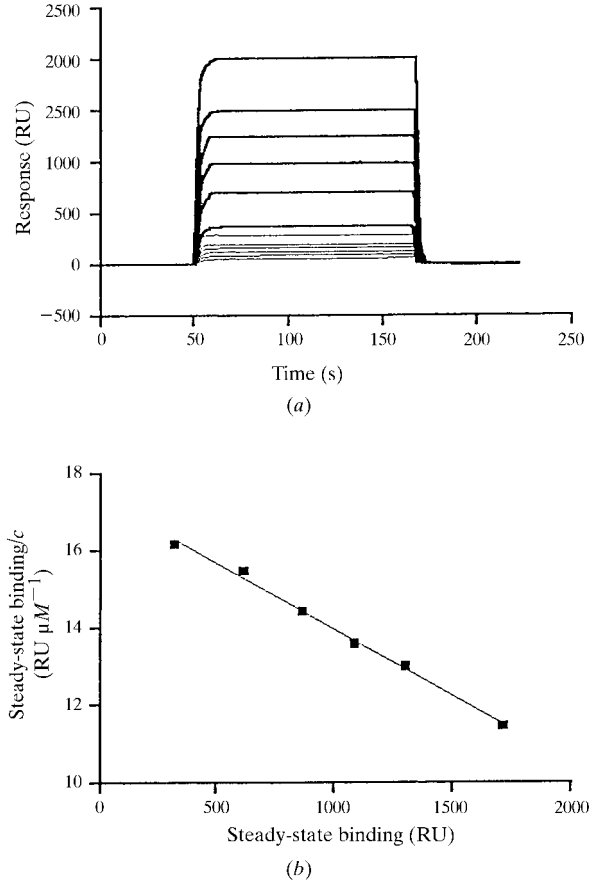

Fig. 2. Analysis of AC1001 binding to a BSA–A-trisaccharide conjugate by surface plasmon resonance. (*a*) Sensorgram overlays showing AC1001 Fv binding to BSA conjugate (thick lines) and control BSA (thin lines) surfaces at concentrations of 20, 40, 60, 80, 100 and 150 µ*M*. (*b*) Scatchard plot of equilibrium binding data obtained by subtraction of control surface from active-surface binding.

Diffraction data were collected for the ligated Fv at room temperature and at 140 K. For the room-temperature data set, a single crystal measuring 0.5 × 0.3 × 0.15 mm was mounted on an Enraf–Nonius FAST area detector located in Dr Louis Delbaere's laboratory at the University of Saskatchewan. The crystals were mounted in glass capillaries with a drop of mother liquor. For the low-temperature data set, several crystals measuring at least 0.4 × 0.2 × 0.1 mm were mounted on an Area Detector Systems Corporation CCD at the A1 station of the MacCHESS facility of the Cornell High Energy Synchrotron Source (CHESS) at Cornell University. Crystals were removed from the hanging drops using rayon loops (Hampton Research) and immediately immersed in cryoprotectant solution for a few seconds. The crystals were then snared again with the rayon loop and placed directly in the nitrogen cooling stream (140 K). The rayon loops were selected to minimize the volume of mother liquor that would be frozen with the drop. The most suitable cryoprotectant was found to be a solution of mother liquor with 20% of the water replaced by glycerol. The frozen drops held in the rayon loops were completely transparent, with no evidence of cracks or stress in the crystals.

3. Results and discussion

3.1. *ScFv isolation and conversion to Fv*

AC1001 scFv obtained by IMAC purification was shown to be homogeneous by SDS–PAGE (data not shown) but was demonstrated to exist in four distinct forms by FPLC SEC (Fig. 1). These peaks correspond to the monomeric, dimeric, trimeric and tetrameric forms of the scFv and arise from V_L–V_H associations involving one to four polypeptide chains. Cleavage of the linker with subtilisin yielded Fv that was homogeneous by SEC with the single peak eluting slightly later than the monomer peak in the scFv preparation (Fig. 1). Both V_L and V_H domains of the Fv could be seen by SDS–PAGE, and failure to detect the V_H domain by Western blotting with the *c-myc* detection antibody indicated at least partial removal of the *c-myc*/His5 extension by protease treatment.

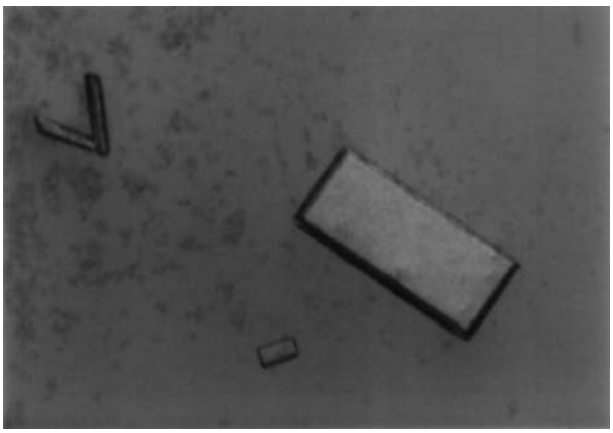

Fig. 3. Photomicrograph of a typical hanging drop containing AC1001 Fv. The large crystal in the centre measures 0.8 × 0.4 × 0.2 mm.

3.2. *Affinity measurements*

The oligosaccharide-binding activity of the Fv was investigated by surface plasmon resonance. Analysis of AC1001Fv binding to a synthetic glycoconjugate, in which the A trisaccharide was attached to BSA through nonyl linkers, showed rapid association and dissociation kinetics (Fig. 2*a*). A comparison of the response on active and control BSA surfaces allowed for subtraction of bulk effects associated with buffer changes and high analyte concentrations and the calculation of specific binding. A Scatchard plot of the specific equilibrium binding data gave a K_D of 290 μM for the interaction (Fig. 2*b*). This value is in good agreement with the 50% inhibition value of 330 μM obtained by Chen & Kabat (1985) by ELISA with the equivalent compound, D-GalNAcα1,3(L-Fucα1,2)-D-Galβ-O$(CH_2)_8COOCH_3$.

3.3. *Diffraction data*

Good-quality large crystals were grown in the presence of GalNAc (Fig. 3). At room temperature, the crystals scattered to 2.2 Å resolution. The unit cell was orthorhombic with $a = 53.6$, $b = 58.5$, $c = 86.1$ Å, $\alpha = \beta = \gamma = 90^\circ$, and the systematic absences were consistent with space group $P2_12_12_1$. The unit cell corresponds to one molecule per asymmetric unit with a V_m of 2.8 Å^3 Da^{-1}. At 140 K, diffraction to 0.93 Å resolution was observed for all crystals of AC1001 Fv; however, sufficient beam time was available to collect a complete data set only to 1.2 Å resolution. The cell dimensions of a = 51.6, b = 58.1, c = 84.3 Å, $\alpha = \beta = \gamma = 90^\circ$ and the systematic absences remained consistent with space group $P2_12_12_1$. 231 724 observations collected between 6.0 and 1.2 Å resolution merged to 68 741 independent reflections using the program *DENZO* (Otwinowski & Minor, 1996), yielding an R_{sym} of 0.048. Of these reflections, 56 657 (82%) were observed with $I \geq 3\sigma(I)$. The final shell (1.24 to 1.20 Å resolution) was 83% complete with an R_{sym} of 0.191. An example diffraction pattern at 140 K is shown in Fig. 4. Unit-cell dimensions and systematic absences did not indicate a change in symmetry in the crystals on going to low temperature, and preliminary molecular-replacement results using the Fv from Fab YsT9.1 as a model (Evans *et al.*, 1994) gave a single strong rotation peak.

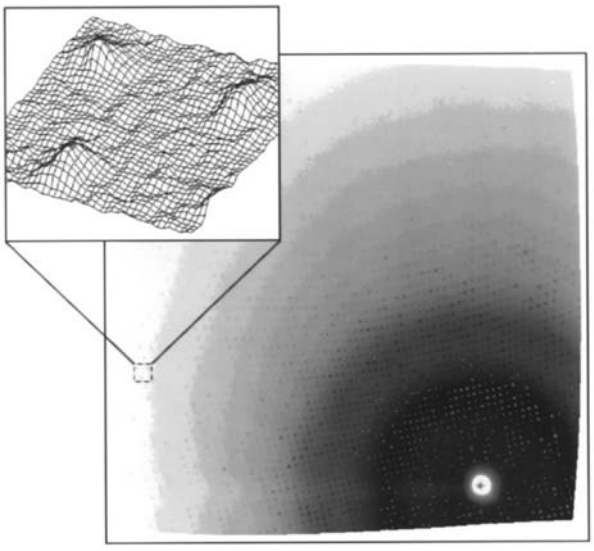

Fig. 4. Raster image from the Area Detector System Corporation CCD area detector at CHESS rendered using the program *ADXV* (Arvai, 1996). The exposure is 5 s with a crystal-to-detector distance of 60 mm. A small portion of reciprocal space is expanded in the top left corner, and shows relief representation of three Bragg reflections from 1.15 to 1.19 Å resolution. Data reduction with *DENZO* (Otwinoski & Minor, 1996) reveals data extending to the extreme edge of the detector (0.93 Å resolution).

We are grateful to MacCHESS (Macromolecular Diffraction at Cornell High Energy Synchrotron Source) staff Joe Navaie, Bill Miller and Marianne Szebenyi for their assistance, and to Les Tari and Dr Louis Delbaere for collecting room-temperature data at the University of Saskatchewan. CHESS is supported by the National Science Foundation under award DMR-9311772, and by award RR-01646 from the National Institutes of Health to MacCHESS. We thank Tomoko Hirama for assistance with the surface plasmon resonance experiments. SVE is supported by a grant from the Natural Sciences and Engineering Research Council of Canada.

References

Al-Lazikani, B., Lesk, A. M. & Chothia, C. (1997). *J. Mol. Biol.* **273**, 927–948.
Arvai, A. (1996). Unpublished work.
Bird, R. E., Hardman, K. D., Jacobson, J. W., Johnson, S., Kaufman, B. M., Lee, S.-M., Lee, T., Pope, S. H., Riordan, G. S. & Whitlow, M. (1988). *Science*, **242**, 423–426.
Chen, H.-T. & Kabat, E. A. (1985). *J. Biol. Chem.* **260**, 13208–13217.
Chen, H.-T., Kabat, E. A., Lundblad, A. & Ratcliffe, R. M. (1987). *J. Biol. Chem.* **262**, 13579–13583.
Chothia, C. & Lesk, A. M. (1987). *J. Mol. Biol.* **196**, 901–917.
Chothia, C., Lesk, A. M., Tramontano, A., Levitt, M., Smith-Gill, S. J., Air, G., Sheriff, S., Padlan, E. A., Davies, D., Tulip, W. R., Colman, P. M., Spinelli, S., Alzari, P. M. & Poljak, R. J. (1989). *Nature (London)*, **342**, 877–883.
Cygler, M., Rose, D. R. & Bundle, D. R. (1991). *Science*, **253**, 442–445.
Evans, S. V., Rose, D. R., To, R. J., Young, N. M. & Bundle, D. R. (1994). *J. Mol. Biol.* **241**, 691–705.
Garratty, G. (1995). *Immunol. Invest.* **24**, 213–232.
Jeffrey, P. D., Bajorath, J., Chang, C. Y., Yelton, D., Hellström, I., Hellström, K. E. & Sheriff, S. (1995). *Nature Struct. Biol.* **2**, 466–471.
King, M.-J. (1994). *Biochim. Biophys. Acta*, **1197**, 15–44.
MacKenzie, C. R., Sharma, V., Brummell, D., Bilous, D., Dubuc, G., Sadowska, J., Young, N. M., Bundle, D. R. & Narang, S. A. (1994). *Biotechnology*, **12**, 390–395.
McPherson, A. J. (1982). *Preparation and Analysis of Protein Crystals*, pp. 82–160. New York: Wiley.
Martin, A. C. & Thornton, J. M. (1996). *J. Mol. Biol.* **263**, 800–815.
Ostermeier, C., Essen, L.-O. & Michel, H. (1995). *Proteins*, **21**, 74–77.
Otwinowski, Z. & Minor, W. (1996). *Methods Enzymol.* **276**, 307–326.
Patenaude, S. I, Vijay, S. M., Yang, Q.-L., Jennings, H. & Evans, S. V. (1998). *Acta Cryst.* D**54**, 1005–1007.
Seymour, G. J., Savage, N. W. & Walsh, L. J. (1995). *Immunology: an Introduction for the Health Sciences*, pp. 109–110. Roseville: McGraw–Hill.
Tizzard, I. R. (1984). *Immunology, an Introduction*, pp. 368–370. Philadelphia: Saunders College Publishing.
Vitali, J., Young, W. W., Schatz, V. B., Sobottka. S. E. & Kretsinger, R. H. (1987). *J. Mol. Biol.* **198**, 351–355.
Zdanov, A., Li, Y., Bundle, D. R., Deng, S.-J., MacKenzie, C. R., Narang, S. A., Young, N. M. & Cygler, M. (1994). *Proc. Natl Acad. Sci. USA*, **91**, 6423–6427.